Inorganic Chemistry

ARTICLE

pubs.acs.org/IC

Synthesis, Electronic Structure, and Catalytic Activity of Reduced Bis(aldimino)pyridine Iron Compounds: Experimental Evidence for Ligand Participation

Sarah K. Russell,[†,§] Carsten Milsmann,[†,§] Emil Lobkovsky,[†] Thomas Weyhermüller,[‡] and Paul J. Chirik*[,†,§]

[†]Department of Chemistry and Chemical Biology, Baker Laboratory, Cornell University, Ithaca, New York 14853, United States

[‡]Max-Planck Institute for Bioinorganic Chemistry, Stiftstrasse 34-36, D-45470 Mülheim an der Ruhr, Germany

Supporting Information

ABSTRACT: The two-electron reduction chemistry of the aryl-substituted bis(aldimino)pyridine iron dibromide, (^{iPr}PDAI)FeBr$_2$ (^{iPr}PDAI = 2,6-(2,6-^{i}Pr$_2$-C$_6$H$_3$−N═CH)$_2$C$_5$H$_3$N), was explored with the goal of generating catalytically active iron compounds and comparing the electronic structure of the resulting compounds to the more well studied ketimine derivatives. Reduction of (^{iPr}PDAI)FeBr$_2$ with excess 0.5% Na(Hg) in toluene solution under an N$_2$ atmosphere furnished the η^6-arene complex, (^{iPr}PDAI)Fe(η^6-C$_7$H$_8$) rather than a dinitrogen derivative. Over time in pentane or diethyl ether solution, (^{iPr}PDAI)Fe(η^6-C$_7$H$_8$) underwent loss of arene and furnished the dimeric iron compound, [(^{iPr}PDAI)Fe]$_2$. Crystallographic characterization established a diiron compound bridged through an η^2-π interaction with an imine arm on an adjacent chelate. Superconducting quantum interference device (SQUID) magnetometry established two high spin ferrous centers each coupled to a triplet dianionic bis(aldimino)pyridine chelate. The data were modeled with two strongly antiferromagnetically coupled, high spin iron(II) centers each with an $S = 1$ [PDAI]$^{2-}$ chelate. Two electron reduction of (^{iPr}PDAI)FeBr$_2$ in the presence of 1,3-butadiene furnished (^{iPr}PDAI)Fe(η^4-C$_4$H$_6$), which serves as a precatalyst for olefin hydrogenation with modest turnover frequencies and catalyst lifetimes. Substitution of the *trans*-coordinated 1,3-butadiene ligand was accomplished with carbon monoxide and *N*,*N*-4-dimethylamino-pyridine (DMAP) and furnished (^{iPr}PDAI)Fe(CO)$_2$ and (^{iPr}PDAI)Fe(DMAP), respectively. The molecular and electronic structures of these compounds were established by X-ray diffraction, NMR and Mössbauer spectroscopy, and the results compared to the previously studied ketimine variants.

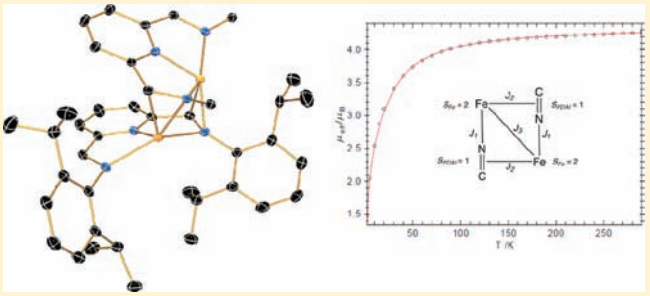

INTRODUCTION

Replacing precious metals with more sustainable, abundant, and potentially nontoxic iron compounds in homogeneous catalysis is an area of widespread interest, and the number of reactions that proceed with high activity and selectivity continues to grow.[1] Much of this recent activity has been inspired by Brookhart and Gibson's independent reports of ethylene and α-olefin polymerization upon activation of aryl-substituted bis(imino)pyridine iron dihalides, (^{R}PDI)FeCl$_2$ (^{R}PDI = 2,6-(*Ar*N═CMe)$_2$C$_5$H$_3$N; *Ar* = 2,6-R$_2$-C$_6$H$_3$; 2,4,6-Me$_3$-C$_6$H$_2$, etc.), with methylaluminoxane (MAO).[2,3] Our laboratory has reported that two electron reduction of these compounds with excess 0.5% sodium amalgam under an N$_2$ atmosphere furnished the corresponding iron dinitrogen complexes, (^{iPr}PDI)Fe(N$_2$)$_2$,[4] (^{iPr}BPDI)Fe(N$_2$)$_2$,[5] and [(^{R}PDI)Fe(N$_2$)]$_2$(μ_2-N$_2$) (R = Et; R = Me; R = Me, ^{i}Pr) (Figure 1).[6] These compounds serve as efficient precatalysts for the hydrogenation of olefins[4,7] with the less sterically protected, dimeric precursors, [(^{R}PDI)Fe(N$_2$)]$_2$(μ_2-N$_2$), exhibiting the higher turnover frequencies.[6] In addition to olefin hydrogenation,[8] (^{iPr}PDI)Fe(N$_2$)$_2$ has been shown to be an effective precatalyst for alkyne hydrogenation,[4] olefin hydrosilylation,[4] the [2π + 2π] cycloisomerization of dienes,[9] and the hydrogenative cyclization of enynes and diynes.[10]

One other notable feature of the aryl-substituted bis(imino)pyridine iron dinitrogen and related neutral ligand compounds is their electronic structures.[11,12] The redox activity of the bis(imino)pyridine chelate,[13−16] the ability to engage in reversible transfer of 1−3 electrons with the metal center,[17,18] often produces metal complexes whose formal oxidation state assignment is deceiving. For example, the neutral ligand compounds, (^{iPr}PDI)Fe-L (L = N$_2$, DMAP,[11] NH$_3$,[19,20] NH$_2$^{t}Bu,[12] etc.), are best described as ferrous compounds with a two-electron reduced bis(imino)pyridine rather than the formal iron(0) alternative. This concept appears general as reduced bis(imino)pyridine ligands have been also been identified in reduced cobalt chemistry.[21−24]

In a continuing effort to improve catalyst performance and to determine the role of redox activity during turnover, our laboratory continues to explore modified tridentate ligand architectures. The presence of ligand centered radicals on the

Received: October 29, 2010
Published: March 11, 2011

 © 2011 American Chemical Society

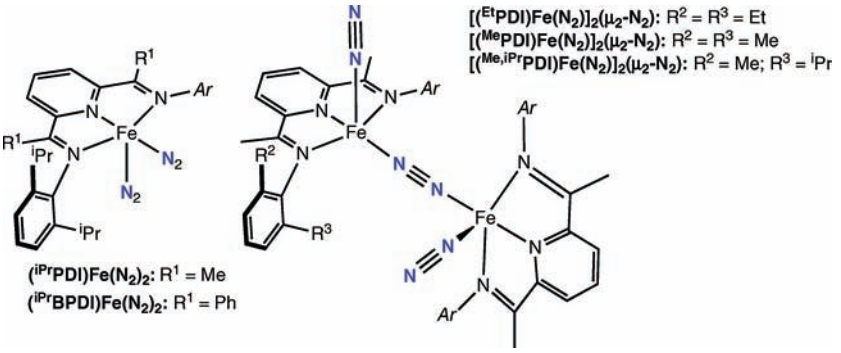

Figure 1. Bis(imino)pyridine iron dinitrogen complexes and their shorthand designations.

bis(imino)pyridine suggests that modifications in the plane of the chelate may alter reactivity and ultimately catalytic performance. Previous studies from our laboratory have demonstrated that replacing the imine methyl groups with phenyl substituents, for example, (^{iPr}PDI)Fe(N_2)$_2$ versus (^{iPr}BPDI)Fe(N_2)$_2$, resulted in a more active 1-hexene hydrogenation catalyst. However, the increased reactivity of the phenylated compound also resulted in shorter catalyst lifetimes as η^6-coordination of the imine aryl groups and the phenyl rings were identified as irreversible deactivation pathways.[5] In ethylene polymerization catalysis, lower activities and molecular weights have been observed when bis(aldimino)pyridine iron dichlorides, for example, (^{iPr}PDAI)-$FeCl_2$ (^{iPr}PDAI = 2,6-(*Ar*N=CH)$_2$C$_5$H$_3$N; *Ar* = 2,6-^{i}Pr$_2$-C$_6$H$_3$) are used in place of the corresponding bis(imino)pyridine compounds.[2a,3a,25,26] Here we describe the differences in the two-electron reduction chemistry between aryl-substituted bis(aldimino)pyridine and bis(imino)pyridine iron dihalide compounds and evaluation of redox activity between the two types of chelates. Notable differences in the isolated iron products and their catalytic performances were found and magnetochemistry on a diiron product provided experimental evidence for the redox activity and triplet diradical character of the bis(aldimino)pyridine supporting ligand.

RESULTS AND DISCUSSION

Reduction of the Bis(aldimino)pyridine Iron Dibromide, (^{iPr}PDAI)FeBr$_2$. The synthetic method used to prepare the ketimine-based bis(imino)pyridine iron dinitrogen complex, (^{iPr}PDI)Fe(N_2)$_2$, was initially explored as a route to the related aldimine-substituted compound. Stirring (^{iPr}PDAI)$FeBr_2$ with excess 0.5% sodium amalgam under a dinitrogen atmosphere did not yield the target iron dinitrogen complex as judged by the absence of N≡N bands in the solution and solid state IR spectra. Analysis of the resulting solid, obtained following filtration and solvent removal, by ^{1}H NMR spectroscopy in benzene-d_6 established formation of a C_s symmetric molecule with an η^6-benzene ligand and a κ^2-bis(aldimino)pyridine chelate (eq 1). Berry and co-workers have reported a related structure in bis(imino)pyridine ruthenium chemistry with the 2,6-dimethyl aryl-variant of the ligand.[27] In the iron chemistry, our laboratory has reported similar 18 electron arene complexes, (^{iPr}DI)Fe(η^6-C_6D_6) and (^{iPr}DI)Fe(η^6-C_7H_8) (^{iPr}DI = (*Ar*N=C(Me)(Me)C=N*Ar*)$_2$; *Ar* = 2,6-^{i}Pr$_2$-C$_6$H$_3$).[28] In the case of the bis(aldimino)pyridine iron compond, 1 equiv of free toluene was observed in the benzene-d_6 ^{1}H NMR spectrum of (^{iPr}PDAI)Fe(η^6-C_6D_6), suggesting that the initial product was the η^6-toluene compound, (^{iPr}PDAI)Fe(η^6-C_7H_8).

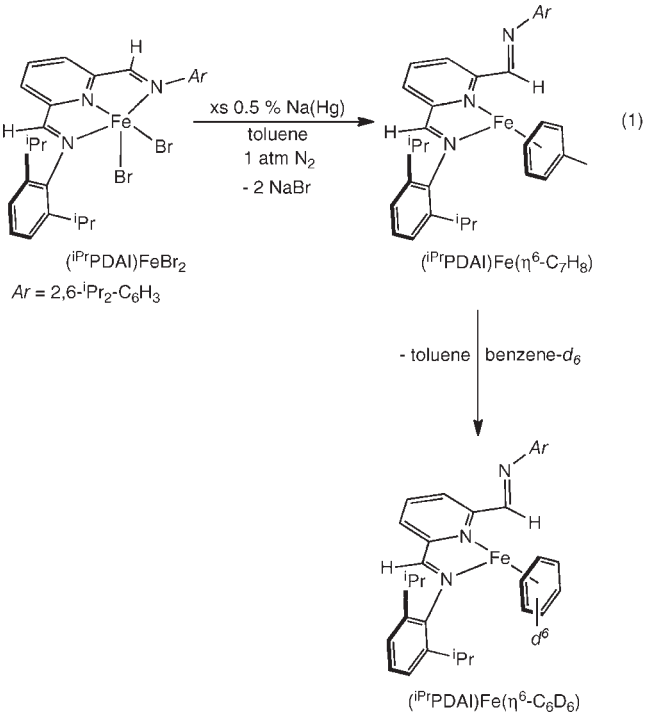

(1)

Attempts to recrystallize (^{iPr}PDAI)Fe(η^6-C_6H_6) or (^{iPr}PDAI)-Fe(η^6-C_7H_8) from diethyl ether, pentane, or a toluene/pentane mixture at −35 °C furnished brown crystals identified as the dimeric iron compound, [(^{iPr}PDAI)Fe]$_2$, in 43% yield (eq 2). Paramagnetic [(^{iPr}PDAI)Fe]$_2$ was also prepared by allowing the arene compounds to stand in nonaromatic solvent for 24 h at 23 °C or by direct reduction of the corresponding iron dibromide, (^{iPr}PDAI)$FeBr_2$, with excess sodium naphthalenide in THF followed by recrystallization from diethyl ether.

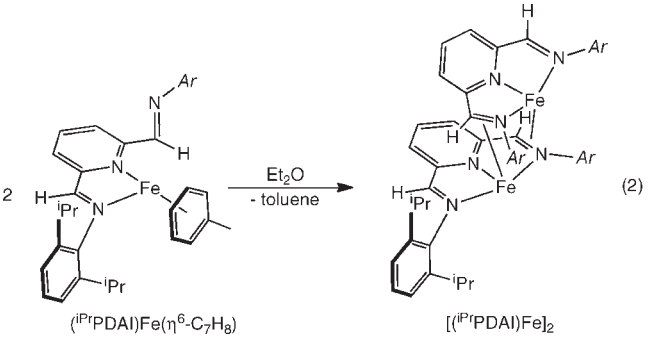

(2)

dx.doi.org/10.1021/ic102186q |*Inorg. Chem.* 2011, 50, 3159–3169

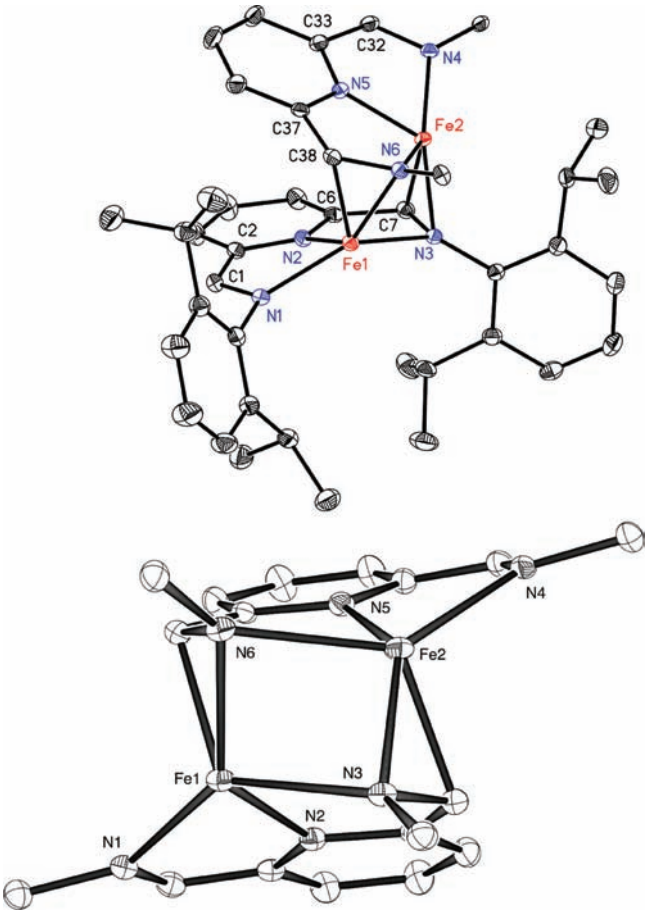

Figure 2. Solid state structure of $[(^{iPr}PDAI)Fe]_2$ at 30% probability ellipsoids. Hydrogen atoms and two aryl groups omitted for clarity (top). Bottom view: All aryl groups removed to highlight the core of the molecule.

The identity of $[(^{iPr}PDAI)Fe]_2$ was established by X-ray diffraction, and a representation of the solid state structure is presented in Figure 2. The unit cell contains a disordered molecule of diethyl ether that reduces the overall quality of the model. Selected bond distances and angles for this compound are reported in Table 1. The crystallographic data for $[(^{iPr}PDAI)Fe]_2$ establish a bimetallic diiron compound with a metal−metal distance of 2.8047(5) Å. An idealized C_2 axis of symmetry passes through the midpoint of the two iron atoms and relates each monomeric subunit of the dimer. The orientation of the isopropyl aryl substituents is responsible for the deviation from idealized symmetry. Each iron atom is five coordinate, ligated by a κ^3-bis(aldimino)chelate and an η^2-C=N imine interaction from the adjacent iron-bis(aldimino)pyridine subunit. The π-interaction with the imine results in deviation of the metal from the idealized κ^3-chelate plane by approximately 20°.

As is well established with bis(imino)pyridines[11,17] and in chemistry of other redox-active ligands,[29−32] bond distortions in the ligand signal non-innocence and participation in the electronic structure. For comparison and reference, the crystal structure of the free ligand, ^{iPr}PDAI, was obtained. A representation of the molecular structure is presented in the Supporting Information, Figure S1. The reference $C_{aldimine}-N_{aldimine}$ distances are 1.265(2) and 1.265(2) Å while those for the $C_{aldimine}-C_{ipso}$ are 1.475(2) and 1.476(2) Å. Caution should be exercised when comparing the ligand bond distances found in $[(^{iPr}PDAI)Fe]_2$ to those of the free chelate or other bis(imino)pyridine compounds as the η^2-C=N imine interaction introduces perturbations not associated with these other molecules. The values in the unperturbed portion of the chelate, N(1)−C(1) and N(4)−C(32), are elongated to 1.326(3) and 1.322(3) Å, respectively while the C(1)−C(2) and C(32)−C(33) bond lengths are contracted to 1.410(3) and 1.412(3) Å, respectively. These values are typically associated with one electron reduction.[33] The imine portion of the bis(aldimino)pyridine chelate involved in bonding to the adjacent iron centers exhibit much larger bond perturbations from the free ligand because of backbonding from the second metal. For example, the N(3)−C(7) and N(6)−C(38) distances are 1.392(3) Å in both cases.

Table 1. Selected Bond Distances (Å) for $[(^{iPr}PDAI)Fe]_2$

	$[(^{iPr}PDAI)Fe]_2$
Fe(1)−N(1)	2.127(2)
Fe(1)−N(2)	1.967(2)
Fe(1)−N(3)	2.272(2)
Fe(1)−N(6)	1.984(2)
Fe(1)−C(38)	2.085(2)
Fe(2)−N(4)	2.149(2)
Fe(2)−N(5)	1.967(2)
Fe(2)−N(6)	2.264(2)
Fe(2)−N(3)	1.983(2)
Fe(2)−C(7)	2.076(2)
N(1)−C(1)	1.326(3)
N(3)−C(7)	1.392(3)
N(4)−C(32)	1.322(3)
N(6)−C(38)	1.392(3)
C(1)−C(2)	1.410(3)
C(6)−C(7)	1.454(4)
C(32)−C(33)	1.412(3)
C(37)−C(38)	1.447(3)
Fe(1)−Fe(2) distance	2.805(5)

The benzene-d_6 ^{1}H NMR spectrum of $[(^{iPr}PDAI)Fe]_2$ exhibits the number of peaks consistent with a C_2 symmetric molecule observed over a 280 ppm chemical shift window. The structure of the dimer is preserved in benzene-d_6 solution as 21 of the expected 23 peaks of the C_2 symmetric dimer were observed. The asymmetry of the bis(aldimino)pyridine ligand in each monomeric subunit gives rise to the larger number of peaks. If the dimer dissociated into a putative three-coordinate iron monomer, benzene coordination would likely be observed; however, no evidence for diamagnetic $(^{iPr}PDAI)Fe(\eta^6\text{-}C_6D_6)$ was obtained by solution NMR spectroscopy at 23 °C.

The electronic structure of $[(^{iPr}PDAI)Fe]_2$ was also studied by zero-field Mössbauer spectroscopy at 80 K. A representative spectrum is presented in Figure 3. Fitting the experimental data yielded an isomer shift (δ) of 0.84 mm/s and a quadrupole splitting (ΔE_Q) of 1.93 mm/s. The isomer shift is comparable to the value of 0.90 mm/s (δ) measured for $(^{iPr}PDAI)FeBr_2$ and is consistent with a high spin iron(II) compound. Thus, both iron centers in $[(^{iPr}PDAI)Fe]_2$ are ferrous, suggesting overall *two* electron reduction of the chelate, one in the unperturbed portion of the chelate and the other in the η^2-imine.

dx.doi.org/10.1021/ic102186q |*Inorg. Chem.* 2011, 50, 3159–3169

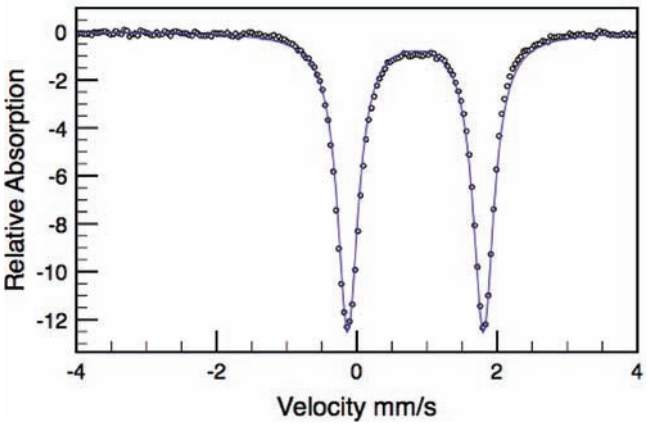

Figure 3. Zero-field ^{57}Fe Mössbauer spectrum of $[(^{iPr}PDAI)Fe]_2$ at 80 K.

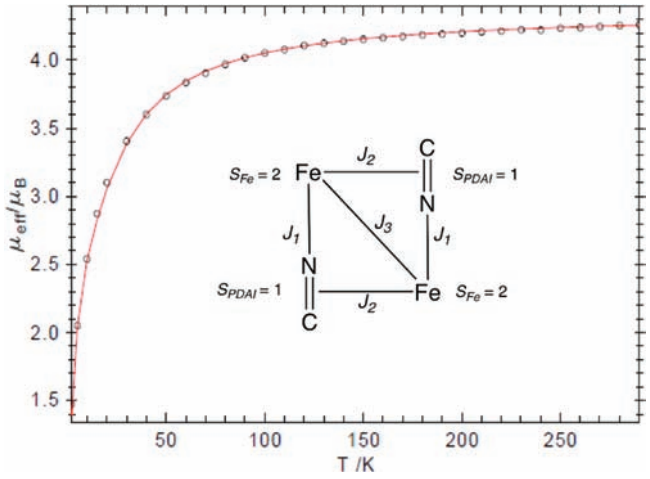

Figure 4. Variable temperature SQUID magnetic data for $[(^{iPr}PDAI)Fe]_2$.

As indicated by its benzene-d_6 ^{1}H NMR spectrum, $[(^{iPr}PDAI)Fe]_2$ is paramagnetic. A solution (benzene-d_6, method of Evans, 293 K) magnetic moment of 4.7 μB was measured for the molecule. A slightly lower value of 4.2 μB was determined in the solid state by magnetic susceptibility balance (296 K). The unusual structural motif observed in the solid state structure of $[(^{iPr}PDAI)Fe]_2$ prompted a more detailed investigation of the magnetochemistry to determine the degree of electronic communication between two iron centers bearing redox-active ligands.

The solid state magnetic behavior of $[(^{iPr}PDAI)Fe]_2$ was studied by superconducting quantum interference device (SQUID) magnetometry, and the temperature dependence of the effective magnetic moment, μ_{eff}, is presented in Figure 4. In the range from 100−300 K μ_{eff} is almost temperature independent and reaches a value of 4.3 μ_B at 300 K, consistent with the magnetic moment of 4.2 μ_B measured at 296 K by magnetic susceptibility balance. Below 100 K, μ_{eff} decreases monotonically from 4.1 μB at 100 K to 1.5 μB at 2 K. The room temperature value of μ_{eff} is very close to the spin only value of 4.0 μ_B for two weakly interacting spins of $S = 1$. On the basis of this information, we modeled the data initially with each $[(^{iPr}PDAI)Fe]$ subunit as a separate $S = 1$ system. While this model readily reproduced the high-temperature region of the data using electronic g values of $g = 2.15$, all attempts to fit the temperature dependence in the low temperature region produced simulation parameters that were physically meaningless. The best fit resulted in a very small isotropic coupling constant, J, of -1.315 cm^{-1}, which is likely too small for a doubly bridged molecule, while the obtained zero field splitting parameter, $|D| = 104$ cm^{-1}, is much larger than reported values for other high spin Fe(II) compounds. To our knowledge, the largest axial zero-field splitting for a high-spin ferrous complex was reported by Münck, Holland, and coworkers for a three-coordinate β-diketiminate iron methyl complex with a value of $|D| = 50$ cm^{-1}.[34] Chang, Long, and coworkers have reported similar values for a family of trigonal pyramidal iron(II) complexes.[35] Furthermore, the large axial zero-field splitting parameters in these compounds can be explained by the particular symmetry of the complexes, which leads to an almost orbitally degenerate ground state with unquenched orbital angular momentum. In contrast, the symmetry around the iron centers in $[(^{iPr}PDAI)Fe]_2$ is significantly lower. Therefore, the unusual parameters led us to investigate a more complicated spin system for the molecule.

The Mössbauer data and metrical parameters from the solid state structure establish two equivalent high spin Fe(II) centers and two $[^{iPr}PDAI]^{2-}$ chelates, respectively. It has been well established[11] that bis(imino)pyridine ligands in their doubly reduced, dianionic form possess nearly degenerate singlet ($S = 0$) and triplet ($S = 1$) states, which have both been identified in coordination compounds.[11,23] Therefore, each high spin Fe(II) center ($S_{Fe} = 2$) and each $[^{iPr}PDAI]^{2-}$ ligand ($S_{PDAI} = 1$) were treated as separate entities, yielding a total of 4 spin centers. The coupling scheme for such a four-spin system in the given geometry and symmetry is presented in the inset in Figure 4. While all coupling pathways are in principle antiferromagnetic in nature, metal−ligand (J_1 and J_2) and metal−metal (J_3) coupling represent competing pathways for the alignment of the spins on the iron centers. Because of the symmetry of the system, the number of independent parameters was significantly reduced by assuming equivalent g and D values for the two iron centers. To further limit the number of fit parameters, g-anisotropy and zero-field splitting were neglected for the ligands ($g_{PDAI} = 2.00$; $|D_{PDAI}| = 0$ cm^{-1}), which is in good agreement with the small deviations from the g value of the free electron and the small zero-field splitting parameters typically observed in organic triplet diradicals.[36,37] The best fit obtained by this model agreed well with the experimental data over the whole temperature range and produced simulation parameters of $|D_{Fe}| = 10.0$ cm^{-1}, $g_{Fe} = 2.11$, $J_1 = -1000$ cm^{-1}, $J_2 = -147$ cm^{-1}, $J_3 = -103$ cm^{-1}.

To further substantiate our model, multiple-field variable-temperature measurements were performed at 1, 4, and 7 T. Reassuringly, the obtained isofield magnetization curves were successfully modeled using the above-mentioned parameters (Supporting Information, Figure S6). However, it should be noted that satisfactory fits to the magnetic susceptibility data were also obtained with different sets of simulation parameters. An analysis of the error surface upon variation of J_2 vs J_3 (all other parameters constant) revealed that even under these strongly constrained conditions no unique solution can be identified, because multiple minima of similar goodness of fit can be found (Supporting Information, Figure S7). Somewhat surprisingly, the values for J_2 and J_3 are also strongly dependent on the magnitude of J_1 (increase in $J_1 \rightarrow$ increase in J_2 and J_3) despite the strength of the antiferromagnetic interaction between the iron and the tridentate ligand in each half of the dimer that precludes

an experimental determination of J_1 by magnetic susceptibility measurements in the accessible temperature range. Although this increases the error of the other variables, the qualitative model remains intact. Very strong antiferromagnetic coupling between each of the high-spin Fe(II) ions with its chelating $[^{iPr}PDAI]^{2-}$ ligand, in agreement with previous results for the ketimine-substituted analogs,[11,23] results in two essentially uncoupled $S = 1$ [(^{iPr}PDAI)Fe] subunits at high temperatures (100−300 K). At lower temperatures, weaker antiferromagnetic coupling between the two subunits gives rise to lower magnetic moments and accounts for the temperature dependence of μ_{eff}. In contrast to J_1 and J_2, which describe the direct magnetic interactions between paramagnetic metal ($S = 2$) and ligand ($S = 1$) fragments, the metal−metal interaction J_3 is mediated via a superexchange pathway. Nevertheless, J_3 is essential within the proposed four-spin coupling model. All simulations employing only the direct interactions J_1 and J_2 resulted in slightly lower fit quality and required large axial zero-field splitting parameters (>50 cm^{-1}) for the iron centers in addition to ferromagnetic coupling constants J_2. Note that because of the competing coupling pathways J_2 and J_3 the effective coupling between the two halves of the dimer is weak, and the compound is paramagnetic over the whole temperature range, despite the sizable antiferromagnetic coupling constants >100 cm^{-1}. In combination with the failure of the simple two spin model to reproduce the low temperature region of the data within reasonable parameters, this model provides strong experimental evidence for the presence of a diradical bis(imino)pyridine ligand coordinated in its triplet state.

Preparation of (^{iPr}PDAI)Fe(η^4-C_4H_6) and (^{iPr}PDAI)Fe(DMAP). To directly compare the electronic structures and ultimately the catalytic activities of reduced bis(aldimino)pyridine iron compounds with their more studied bis(imino)pyridine iron counterparts, compounds with identical metal−ligand combinations were targeted. In bis(imino)pyridine iron chemistry, reduction of the iron dihalide precursor in the presence of 1,3-butadiene has proven to be a reliable and straightforward method for synthesis of precatalysts for iron-catalyzed olefin hydrogenation[9] even when the corresponding dinitrogen complex is synthetically inaccessible. In addition, the solid state structure of (^{iPr}PDI)Fe(η^4-C_4H_6) established the *trans* geometry of the butadiene ligand.[9,38] Synthesis of the target (^{iPr}PDAI)Fe(η^4-C_4H_6) compound was accomplished by stirring a pentane slurry of (^{iPr}PDAI)$FeBr_2$ with excesses of both 0.5% Na(Hg) (~3 equiv) and 1,3-butadiene (~10 equiv). Filtration and recrystallization from diethyl ether at −35 °C yielded a brown solid in 70% isolated yield (eq 3).

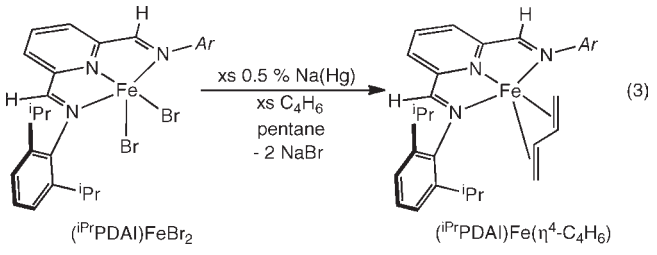

(3)

The benzene-d_6 ^{1}H NMR spectrum of (^{iPr}PDAI)Fe(η^4-C_4H_6) at 20 °C exhibits the number of resonances consistent with a C_2 symmetric molecule. Notably, all of the resonances are broad, suggesting a dynamic process on the time scale of the spectroscopic experiment. Cooling a toluene-d_8 solution of the compound to temperatures below −20 °C resulted in a sharpening of the bis(imino)pyridine resonances while those for the butadiene remain slightly broadened (see Supporting Information, Figure S4, for a stack plot), suggesting that the dynamic process involves dissociation and recoordination of the diene. Warming the sample above 40 °C produced the number of resonances consistent with a C_{2v} symmetric molecule with only two observable butadiene peaks, demonstrating that the exchange process is faster than the NMR time scale.

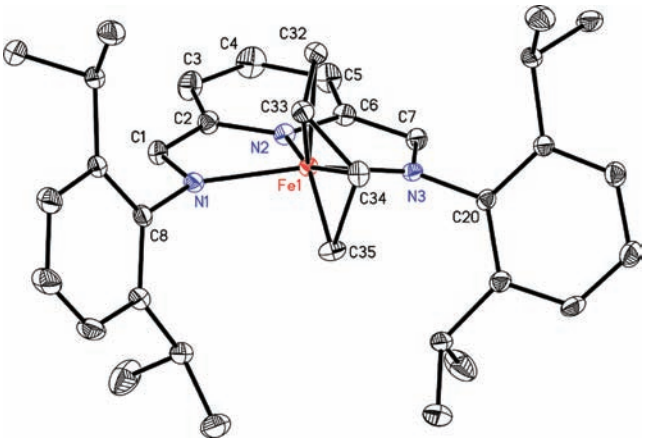

Figure 5. Solid state structure of (^{iPr}PDAI)Fe(η^4-C_4H_6) at 30% probability ellipsoids. Hydrogen atoms omitted for clarity.

Table 2. Selected Bond Distances (Å) and Angles (deg) for (^{iPr}PDAI)Fe(η^4-C_4H_6) and (^{iPr}PDI)Fe(η^4-C_4H_6)[a]

	(^{iPr}PDAI)Fe(η^4-C_4H_6)	(^{iPr}PDI)Fe(η^4-C_4H_6)
Fe−N_{py}	1.852(2)	1.841(7)
Fe−N_{imine}	1.966(2), 1.979(2)	2.005(1), 1.966(1)
Fe−C_{CH2}	2.129(2), 2.240(1)	2.179(2), 2.196(1)
Fe−C_{CH}	2.041(3), 2.055(3)	2.050(1), 2.057(1)
N_{imine}−C_{imine}	1.329(3), 1.333(3)	1.332(1), 1.372(1)
C_{imine}−C_{ipso}	1.410(3), 1.402(3)	1.422(1), 1.414(1)

[a] Data taken from reference 9.

The solution dynamic behavior of the η^4-butadiene ligand in (^{iPr}PDAI)Fe(η^4-C_4H_6) prompted a similar investigation of the previously reported ketimine-substituted compound for comparison.[9] The benzene-d_6 solution ^{1}H NMR spectrum of (^{iPr}PDI)Fe(η^4-C_4H_6) at 20 °C exhibits the number of resonances consistent with a molecule of C_2 molecular symmetry. Importantly, these resonances are sharper than those of the corresponding aldimine complex, (^{iPr}PDAI)Fe(η^4-C_4H_6), under identical conditions, suggesting a higher barrier for the dynamic process involving the butadiene ligand. Warming the solution to 40 °C resulted in a broadening of the bis(imino)pyridine and diene resonances, further supporting a higher barrier for dissociation and recoordination in the ketimine substituted compound as compared to its aldimine counterpart.

Single crystals of (^{iPr}PDAI)Fe(η^4-C_4H_6) suitable for X-ray diffraction were obtained from a concentrated hexane solution cooled to −35 °C. A representation of the solid state molecular structure is presented in Figure 5 and selected bond distances are reported in Table 2. Also presented in Table 2 are the distances for the analogous bis(imino)pyridine iron butadiene compound, (^{iPr}PDI)Fe(η^4-C_4H_6). The overall molecular geometry of

dx.doi.org/10.1021/ic102186q |*Inorg. Chem.* 2011, 50, 3159–3169

(^{iPr}PDI)Fe(η^4-C_4H_6) is similar to (^{iPr}PDAI)Fe(η^4-C_4H_6) with both compounds containing a relatively unusual *trans*-butadiene ligand.[39,40] The bond distances in the bis(aldimino)chelate are consistent with two electron reduction and indicate a ferrous oxidation state. The distortions in $N_{imine}-C_{imine}$ and $C_{imine}-C_{ipso}$ bond distances are comparable to the bis(imino)pyridine variant with a slightly more pronounced $C_{imine}-C_{ipso}$ contraction for the aldimino example. The butadiene ligand of the bis(aldimino)pyridine complex is less symmetrically bound to the iron center with one shorter and one longer $Fe-C_{CH2}$ bond in comparison to the bis(imino)pyridine complex which has two very similar $Fe-C_{CH2}$ bond distances.

To further explore electronic structure differences between reduced aryl-substituted bis(aldimino)pyridine and bis(imino)pyridine iron compounds, other neutral ligand derivatives of [(^{iPr}PDAI)Fe] were targeted. Two specific examples, (^{iPr}PDAI)Fe(CO)$_2$ and (^{iPr}PDAI)Fe(DMAP) (DMAP = *N*,*N*-4-dimethylaminopyridine), were selected because of the extensive spectroscopic and computational studies carried out on the corresponding bis(imino)pyridine derivatives.[11,12] Synthesis of the dicarbonyl compound, (^{iPr}PDAI)Fe(CO)$_2$, was accomplished by addition of one atmosphere of carbon monoxide to the iron butadiene compound (^{iPr}PDAI)Fe(η^4-C_4H_6) and furnished the desired product as a green solid in 92% yield (eq 4). This molecule was also prepared from direct sodium amalgam reduction of (^{iPr}PDAI)-$FeBr_2$ in the presence of excess carbon monoxide.

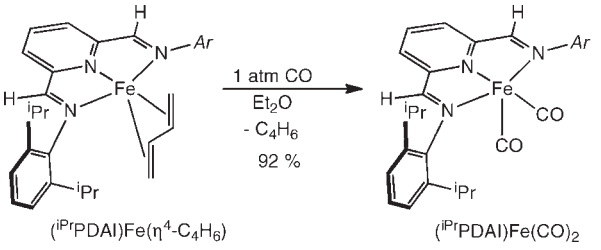

(4)

Diamagnetic (^{iPr}PDAI)Fe(CO)$_2$ was characterized by multinuclear NMR, solution IR, and solid state zero-field Mössbauer spectroscopies. The benzene-d_6 ^{1}H and ^{13}C NMR spectra exhibit the number of peaks expected for a C_{2v} symmetric molecule, consistent with rapid exchange between the carbonyl ligands on the NMR time scale. The pentane solution infrared spectrum of (^{iPr}PDAI)Fe(CO)$_2$ exhibits two strong carbonyl bands centered at 1981 and 1925 cm^{-1}. These values are at modestly higher energy than those (ν_{CO} = 1974, 1914 cm^{-1}) for (^{iPr}PDI)Fe(CO)$_2$[4] demonstrating that the ketimine-substituted complex has a slightly more electron rich iron center than the corresponding aldimine compound.

The synthesis of the other targeted neutral ligand derivative, (^{iPr}PDAI)Fe(DMAP), was also accomplished from the corresponding butadiene compound. Addition of 1 equiv of DMAP to a diethyl ether solution of (^{iPr}PDI)Fe(η^4-C_4H_6) furnished a brown solid identified as (^{iPr}PDAI)Fe(DMAP) in 95% isolated yield (eq 5).

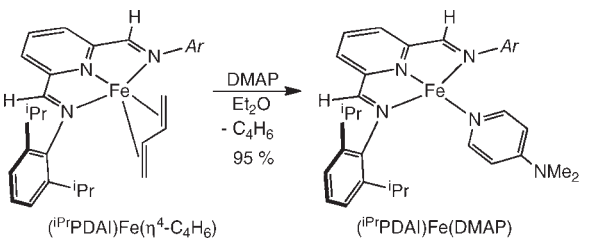

(5)

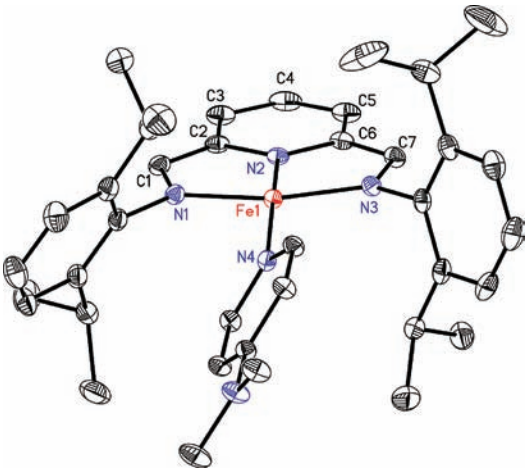

Figure 6. Solid state structure of (^{iPr}PDAI)Fe(DMAP) at 30% probability ellipsoids. Hydrogen atoms omitted for clarity.

Table 3. Selected Bond Distances (Å) and Angles (deg) for (^{iPr}PDAI)Fe(DMAP) and (^{iPr}PDI)Fe(DMAP)[a]

	(^{iPr}PDAI)Fe(DMAP)	(^{iPr}PDI)Fe(DMAP)
$Fe-N_{py}$	1.836(2)	1.821(3)
	1.833(2)	
$Fe-N_{imine}$	1.904(2), 1.922(2)	1.908(3), 1.943(3)
	1.889(2), 1.917(2)	
$Fe-N_{DMAP}$	1.978(2)	1.979(3)
	1.985(2)	
$N_{imine}-C_{imine}$	1.339(3), 1.355(3)	1.350(5), 1.358(5)
	1.349(3), 1.343(3)	
$C_{imine}-C_{ipso}$	1.407(4), 1.406(4)	1.414(5), 1.406(5)
	1.406(3), 1.406(3)	
$C_{ipso}-N_{py}$	1.379(3), 1.373(3)	1.390(5), 1.387(5)
	1.382(3), 1.376(3)	

[a] Data taken from reference 11.

The electronic structure of (^{iPr}PDI)Fe(DMAP) was determined previously and is best described as an intermediate spin ferrous compound antiferromagnetically coupled to a bis(imino)pyridine diradical dianion.[11] The benzene-d_6 ^{1}H and ^{13}C NMR spectra of diamagnetic (^{iPr}PDI)Fe(DMAP) exhibit unusual shifts of the in-plane chelate resonances that signal temperature independent paramagnetism arising from mixing of singlet and triplet states via spin orbit coupling. For example, in the ^{1}H NMR spectrum, the imine methyl groups are shifted upfield to −5.85 ppm while the *meta*- and *para*-pyridine hydrogens were located at 12.42 and 9.04 ppm, respectively. Importantly, these resonances do not shift dramatically as a function of temperature supporting TIP rather than contributions from thermal population of paramagnetic excited states or from contamination by paramagnetic iron impurities. The benzene-d_6 ^{1}H NMR spectrum of the aldimine variant, (^{iPr}PDAI)Fe(DMAP), exhibits the number of peaks for an idealized C_2 symmetric molecule. Notable features include a substantially downfield shifted aldimine hydrogen centered at 17.16 ppm and the *meta*- and *para*-pyridine hydrogens at 12.66 and 8.50 ppm, respectively. For context, the aldimine hydrogen appears at 8.54 ppm in the free ligand and at 8.20 ppm in the diamagnetic iron dicarbonyl compound, (^{iPr}PDAI)Fe(CO)$_2$. Accordingly, the *meta*-pyridine hydrogens appear at 8.30 and 7.62 ppm in the free ligand and the dicarbonyl compound, respectively. The

dx.doi.org/10.1021/ic102186q |*Inorg. Chem.* 2011, 50, 3159–3169

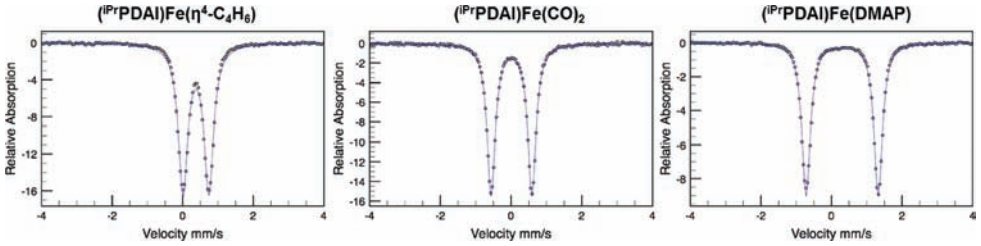

Figure 7. Representative zero-field Mössbauer spectra for (^{iPr}PDAI)Fe(η^4-C_4H_6), and (^{iPr}PDAI)Fe$(CO)_2$ and (^{iPr}PDAI)Fe(DMAP) recorded at 80 K.

corresponding *para*-pyridine values are 7.19 and 7.16 ppm, respectively. Variable temperature NMR experiments in toluene-d_8 solution produce little change in the chemical shift of these resonances. For example, the aldimine hydrogen moves approximately 4 ppm over a 120 °C temperature range. At −40 °C, this peak is located at 18.95 ppm and shifts upfield to 14.68 ppm upon warming to 80 °C. This shift is larger than what would be expected from a pure diamagnetic compound (without mixing of excited states) yet smaller than that anticipated for a simple paramagnetic compound obeying the Curie−Weiss law.

Single crystals of (^{iPr}PDAI)Fe(DMAP) were obtained from a concentrated diethyl ether solution cooled to −35 °C. Two molecules are present in the asymmetric unit and differ by the direction of rotation of the DMAP ligand with respect to the iron-chelate plane. A representation of the solid state structure of one of the molecules is presented in Figure 6, and selected bond distances and angles for both are reported in Table 3. Also included in Table 3 are the corresponding values for (^{iPr}PDI)Fe(DMAP) for comparison. The overall molecular geometry of the iron in (^{iPr}PDAI)Fe(DMAP) is best described as idealized square planar with the plane of the *N*,*N*-dimethylaminopyridine ligand canted at 53.78(6)° and 55.36(6)° with respect to the iron chelate plane. This value is 50.36(10)° in the ketimine compound, (^{iPr}PDI)Fe(DMAP).

The distortions to the chelate in the solid state structure of (^{iPr}PDAI)Fe(DMAP) are consistent with two electron reduction and hence an intermediate spin ferrous compound, analogous to the electronic structure previously determined for (^{iPr}PDI)Fe(DMAP).[11] In one of the molecules, the $N_{imine}-C_{imine}$ bonds are elongated to 1.339(3) and 1.355(3) Å while in the other these values are 1.349(3), 1.343(3) Å, longer than the values in $[(^{iPr}PDAI)Fe]_2$, where one electron reduction of the unperturbed portion of the chelate was observed. Likewise, the $C_{imine}-C_{ipso}$ bond distances are contracted to 1.407(4) and 1.406(4) Å in one molecule and to 1.406(3) and 1.406(3) Å in the other. These distortions are comparable and in some instances more pronounced that in the ketimine compound. The iron−nitrogen bond distances in (^{iPr}PDAI)Fe(DMAP) also establish an intermediate rather than high spin ferrous compound. Short $Fe-N_{pyr}$ distances of 1.836(2) and 1.833(2) Å are observed along with contracted $Fe-N_{imine}$ bonds of 1.904(2), 1.922(2), 1.889(2), and 1.917(2) Å. In analogous high spin compounds, the latter values are typically over 2.0 Å.

The electronic structures of (^{iPr}PDAI)Fe(η^4-C_4H_6), (^{iPr}PDAI)Fe$(CO)_2$, and (^{iPr}PDAI)Fe(DMAP) were also investigated by zero-field ^{57}Fe Mössbauer spectroscopy. Representative spectra are reported in Figure 7, and the experimental parameters for these and the corresponding ketimine compounds are presented in Table 4. For each compound, there is little difference in the isomer shift (δ) and quadrupole splitting (ΔE_Q) between the aldimine- and the ketimine-substituted compounds, indicating similar electronic environments at each iron center. For the butadiene and DMAP derivatives, the isomer shifts are consistent with intermediate spin ferrous compounds[11] while for the carbonyl compounds the lower value of δ indicates a higher degree of covalency and contributions from Fe(0).

Table 4. Zero-Field Mössbauer Parameters for (^{iPr}PDAI)Fe(η^4-C_4H_6) and (^{iPr}PDAI)Fe(DMAP) Determined at 80 K[a]

	δ (mm/s)	ΔE_Q (mm/s)
(^{iPr}PDAI)Fe(η^4-C_4H_6)	0.37	0.73
(^{iPr}PDI)Fe(η^4-C_4H_6)	0.38	0.38
(^{iPr}PDAI)Fe$(CO)_2$	0.01	1.15
(^{iPr}PDI)Fe$(CO)_2$	0.03	1.17
(^{iPr}PDAI)Fe(DMAP)	0.30	2.04
(^{iPr}PDI)Fe(DMAP)	0.31	1.94

[a] Data is also included for the analogous bis(imino)pyridine iron compounds for comparison. For (^{iPr}PDI)Fe$(CO)_2$ and (^{iPr}PDI)Fe(DMAP) the data were taken from ref 11.

Evaluation in Catalytic Olefin Hydrogenation. The synthesis of reduced bis(aldimino)pyridine iron compounds prompted evaluation of their catalytic performance. The analogous bis(imino)pyridine iron dinitrogen complexes are highly active catalysts for olefin hydrogenation,[4−7] hydrosilylation,[4,5] and cycloisomerization reactions.[9,10] In a recent study with the ketimine-substituted compounds, the hydrogenation of ethyl-3-methylbut-2-enoate was used as a representative model substrate to evaluate the effect of changes in catalyst structure on the efficiency and lifetime of turnover. This substrate was also used in this study to determine differences between aldimine- and ketimine-substituted iron precatalysts (eq 6). It should be noted that the originally reported iron bis(dinitrogen) compound, (^{iPr}PDI)Fe$(N_2)_2$, reaches only 65% conversion to product after 72 h after which time the iron is deactivated by irreversible C−O bond cleavage.[7,41] Full conversion is obtained when the aryl groups are reduced to ethyl or methyl substituents. In each of the precatalyst screening experiments described in this study, standard conditions were employed where a 0.92 M solution of substrate was prepared in benzene-d_6 along with 5 mol % of the iron precatalyst and four atmospheres of dihydrogen. The progress of the reaction was then evaluated using ^{1}H NMR spectroscopy.

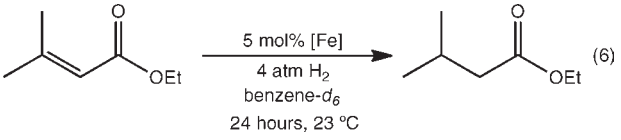

(6)

dx.doi.org/10.1021/ic102186q |*Inorg. Chem.* 2011, 50, 3159–3169

Attempts to hydrogenate ethyl-3-methylbut-2-enoate with $[(^{iPr}PDAI)Fe]_2$ under standard conditions outlined in the preceding paragraph produced no turnover after days at 23 °C. In an attempt to observe catalytic turnover, a similar experiment was performed with cyclohexene as the substrate. Previous studies with the ketimine precatalyst, $(^{iPr}PDI)Fe(N_2)_2$, established much more rapid hydrogenation of the unactivated alkene. Once again, no turnover was observed after 2 days, demonstrating that $[(^{iPr}PDAI)Fe]_2$ is not an effective hydrogenation precatalyst nor does it dissociate in solution to a catalytically active species. As an alternative, $(^{iPr}PDAI)Fe(\eta^4\text{-}C_4H_6)$ was explored with the goal of hydrogenating the coordinated olefin to generate an active iron catalyst. For comparison, the corresponding bis(imino)-pyridine iron butadiene complex, $(^{iPr}PDI)Fe(\eta^4\text{-}C_4H_6)$,[9] was also studied. Each catalytic hydrogenation of ethyl-3-methylbut-2-enoate was carried out for 24 h and the conversion to product determined by ^{1}H NMR spectroscopy. The ketimine-substituted precatalyst, $(^{iPr}PDI)Fe(\eta^4\text{-}C_4H_6)$, produced 60% conversion after this time interval, comparable to the 65% conversion reported for the iron bis(dinitrogen) precatalyst, $(^{iPr}PDI)Fe(N_2)_2$.[6,7] By comparison, the aldimine-substituted iron butadiene compound, $(^{iPr}PDAI)Fe(\eta^4\text{-}C_4H_6)$, reached only 20% conversion after 24 h. Running the reaction for 48 h improved the conversion to 35% but no additional turnover was observed at longer reaction times. With cyclohexene as the substrate, the ketimine complex, $(^{iPr}PDI)Fe(\eta^4\text{-}C_4H_6)$ reached >99% conversion after 1 h while the aldimine compound, $(^{iPr}PDAI)Fe(\eta^4\text{-}C_4H_6)$, produced only 28% conversion after 4 h, finally reaching >99% conversion after 24 h.

Additional studies were conducted to determine the origin of the poor catalytic performance of the aldimine-substituted iron butadiene compound. Treatment of a benzene-d_6 solution of $(^{iPr}PDAI)Fe(\eta^4\text{-}C_4H_6)$ with 4 atm of dihydrogen resulted in loss of butane over the course of days at 23 °C with concomitant formation of the iron benzene complex, $(^{iPr}PDAI)Fe(\eta^6\text{-}C_6D_6)$ (eq 7). Accordingly, analysis of the iron compound following catalytic hydrogenation of cyclohexene by ^{1}H NMR spectroscopy established formation of $(^{iPr}PDAI)Fe(\eta^6\text{-}C_6D_6)$ along with other unidentified (both diamagnetic and paramagnetic) iron compounds. No evidence for formation of $[(^{iPr}PDAI)Fe]_2$ was obtained by ^{1}H NMR spectroscopy following these experiments or hydrogenations conducted in aliphatic hydrocarbon solvent. Catalyst recycling experiments were also conducted whereby the hydrogenation of cyclohexene was conducted in benzene-d_6 with 5 mol % of $(^{iPr}PDAI)Fe(\eta^4\text{-}C_4H_6)$ and run to >95% conversion. The reaction was then recharged with another 20 equiv of cyclohexene (per original amount of $(^{iPr}PDAI)Fe(\eta^4\text{-}C_4H_6)$) and 4 atm of H_2 added. After 16 h, 40% conversion to alkane was observed. For comparison, 82% conversion was observed with the original charge after 16 h, suggesting competing catalyst deactivation.

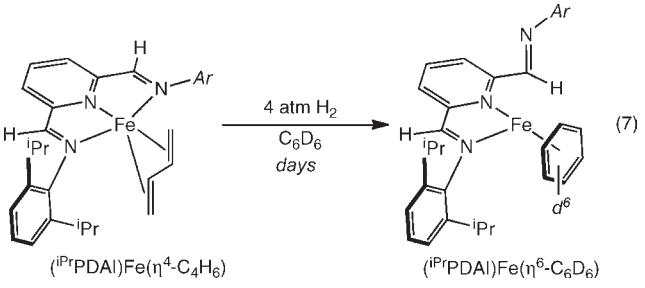

(7)

$(^{iPr}PDAI)Fe(\eta^4\text{-}C_4H_6)$ $(^{iPr}PDAI)Fe(\eta^6\text{-}C_6D_6)$

By comparison, the ketimine-substituted iron butadiene compound $(^{iPr}PDI)Fe(\eta^4\text{-}C_6H_6)$ undergoes complete conversion to the corresponding dihydrogen compound $(^{iPr}PDI)Fe(\eta^2\text{-}H_2)^4$ overnight. Therefore, the difference in hydrogenation activity between the two complexes can be traced, in part, to the slower initiation of the aldimine iron butadiene compound relative to its ketimine counterpart and also to the catalyst deactivation by coordination of the arene solvent. As a result, the relatively more open coordination sphere around the iron in the aldimine complex does not improve catalysis but rather inhibits it by slowing the likely dissociative precatalyst activation processes and enabling competing deactivation pathways.

CONCLUDING REMARKS

The chemistry of reduced aryl-substituted bis(aldimino)-pyridine complexes has been explored and compared to their more studied ketimine counterparts. Two electron reduction of the iron dibromide precursor in aromatic solvents such as benzene or toluene furnished substitutionally labile bis-(aldimino)pyridine arene complexes. Over time in aliphatic hydrocarbon or ethereal solvents, these compounds converted to the diiron complex, $[(^{iPr}PDAI)Fe]_2$, where each iron is bridged via an η^2-interaction with an imine group on an adjacent chelate. Mössbauer spectroscopy established two high spin ferrous centers, and modeling the variable temperature magnetochemical data provided experimental evidence for diradical character on the bis(aldimino)chelate. Both arene coordination and dimerization in lieu of dinitrogen coordination contrast the known chemistry for analogous ketimine-substituted bis-(imino)pyridine compounds and suggest that the iron center in the aldimine variants is less sterically protected. Performing the reduction of the iron dibromide in the presence of 1,3-butadiene yielded the diamagnetic diene compound, $(^{iPr}PDAI)Fe(\eta^4\text{-}C_4H_6)$, which serves as catalyst precursor for olefin hydrogenation as well as a synthetic precursor for the iron dicarbonyl, $(^{iPr}PDAI)Fe(CO)_2$, and 4-*N*,*N*-dimethylaminopyridine, $(^{iPr}PDAI)Fe(DMAP)$, derivatives. The carbonyl stretching frequencies of $(^{iPr}PDAI)Fe(CO)_2$ establish a slightly less electron rich iron center than the corresponding ketimine-substituted bis(imino)pyridine compound, but Mössbauer spectroscopy on all compounds established little change in the overall electronic structure. The relatively poor catalytic performance of the aldimine precursor was traced to the more open coordination environment around the iron center, resulting in slower pre-catalyst activation reactions and enabling catalyst deactivation events.

EXPERIMENTAL SECTION

General Considerations. All air- and moisture-sensitive manipulations were carried out using standard vacuum line, Schlenk, and cannula techniques or in an MBraun inert atmosphere drybox containing an atmosphere of purified nitrogen. Solvents for air- and moisture-sensitive manipulations were dried and deoxygenated using literature procedures.[42] Benzene-d_6 was purchased from Cambridge Isotope Laboratories, distilled from Na metal, and dried over 4 Å molecular sieves.

^{1}H NMR spectra were recorded on Varian Mercury 300, Inova 400, 500, and 600 spectrometers operating at 299.76, 399.78, 500.62, and 599.78 MHz, respectively. ^{13}C NMR spectra were recorded on an Inova 500 spectrometer operating at 125.893 MHz. All ^{1}H and ^{13}C NMR chemical shifts are reported relative to $SiMe_4$ using the ^{1}H (residual) and

^{13}C chemical shifts of the solvent as a secondary standard. Infrared spectra were collected on a Thermo Nicolet spectrometer. Elemental analyses were performed at Robertson Microlit Laboratories, Inc., in Madison, NJ.

Single crystals suitable for X-ray diffraction were coated with polyisobutylene oil in a drybox, transferred to a nylon loop, and then quickly transferred to the goniometer head of a Bruker X8 APEX2 diffractometer equipped with a molybdenum X-ray tube (λ = 0.71073 Å). Preliminary data revealed the crystal system. A hemisphere routine was used for data collection and determination of lattice constants. The space group was identified and the data were processed using the Bruker SAINT+ program and corrected for absorption using SADABS. The structures were solved using direct methods (SHELXS) completed by subsequent Fourier synthesis and refined by full-matrix least-squares procedures.

Zero-field ^{57}Fe Mössbauer spectra were recorded on a SEE Co. Mössbauer spectrometer (MS4) at 80 K in constant acceleration mode. ^{57}Co/Rh was used as the radiation source. WMOSS software was used for the quantitative evaluation of the spectral parameters (least-squares fitting to Lorentzian peaks). The minimum experimental line widths were 0.23 mm s^{-1}. The temperature of the sample was controlled by a Janis Research Co. CCS-850 He/N_2 cryostat within an accuracy of ±0.3 K. Isomer shifts were determined relative to α-iron at 298 K.

SQUID magnetization data of crystalline powdered samples were recorded with a SQUID magnetometer (Quantum Design) at 10 kOe between 5 and 300 K for all samples. Values of the magnetic susceptibility were corrected for the underlying diamagnetic increment by using tabulated Pascal constants and the effect of the blank sample holders (gelatin capsule/straw). Samples used for magnetization measurement were recrystallized multiple times and checked for chemical composition by ^{1}H NMR and Mössbauer spectroscopy. The program julX written by E. Bill was used for the simulation and analysis of magnetic susceptibility data.[43]

Preparation of (^{iPr}PDAI)FeBr$_2$. A 100 mL round-bottom flask was charged with 1.55 g (3.42 mmol) of ^{iPr}PDAI and 0.736 g (3.41 mmol) of $FeBr_2$. Approximately 20 mL of tetrahydrofuran (THF) was added, and the resulting reaction mixture was stirred for 16 h producing a green solution. Pentane (50 mL) was then added to the flask, and blue solid precipitated. The solid was collected by filtration and yielded 2.12 g (93%) of a dark blue powder identified as (^{iPr}PDAI)$FeBr_2$. Analysis for $C_{31}H_{39}N_3FeBr_2$: Calcd C, 55.63; H, 5.87; N, 6.28. Found C, 55.51; H, 5.90; N, 6.16. ^{1}H NMR (CD_2Cl_2): δ = −8.07 (22 Hz), −0.67 (156 Hz, 24H, CH(CH_3)$_2$), 1.55 (9 Hz) 1.82 (14 Hz), 3.69 (14 Hz), 14.71 (24 Hz), 59.88 (44 Hz).

Preparation of (^{iPr}PDAI)Fe(η^6-C_7H_8). A 100 mL round-bottom flask was charged with 9.0 g (45 mmol) of mercury and approximately 15 mL of toluene. Sodium metal (0.045 g, 1.96 mmol) was added, and the slurry was amalgamated for 10 min. Solid (^{iPr}PDAI)$FeBr_2$ (0.500 g, 0.747 mmol) was added followed by approximately 5 mL of diethyl ether. Within 10 min the color of the solution changed from blue to green to brown. Approximately 2 min after the color had reached a constant brown color, the solution was decanted from the amalgam and then filtered through Celite. The amalgam was washed with pentane, and the wash filtered through Celite. Removal of all solvent and collection of the crude material yielded 0.365 g (81%) of a brown solid identified as (^{iPr}PDAI)Fe(η^6-C_7H_8). Dissolution in C_6D_6 resulted in immediate displacement of the η^6-bound toluene ligand with a molecule of C_6D_6 and formation of (^{iPr}PDAI)Fe(η^6-C_6H_6) and 1 equiv of free toluene. ^{1}H NMR (toluene-d_8): δ = 0.92 (d, 6.8 Hz, 6H, CH(CH_3)$_2$), 1.32 (d, 6.8 Hz, 12H, CH(CH_3)$_2$), 1.41 (d, 6.8 Hz, 6H, CH(CH_3)$_2$), 3.40 (q, 6.8 Hz, 2H, CH(CH$_3$)$_2$), 3.55 (q, 6.8 Hz, 2H, CH(CH$_3$)$_2$), 6.60 (d, 8.0 Hz, 1H, *m-py*), 6.71 (t, 8.0 Hz, 1H, *p-py*), 7.08 (s, 1H, N=CH), 7.18 (d, 2H, 7.6 Hz, *m-Ar*), 7.22 (d, 2H, 7.6 Hz, *m-Ar*), 7.32 (t, 2H, 7.6 Hz, *p-Ar*), 7.70 (d, 8.0 Hz, 1H, *m-py*), 9.70 (s, 1H, N=CH).

Preparation of (^{iPr}PDAI)Fe(η^6-C_6H_6). This compound was prepared in a similar manner to (^{iPr}PDAI)Fe(η^6-C_7H_8) with 0.500 g (0.747 mmol) of (^{iPr}PDAI), 0.45 g Na in 9.0 g of Hg and approximately 15 mL of benzene. This procedure yielded 0.341 g (78%) of a brown solid identified as (^{iPr}PDAI)Fe(η^6-C_6H_6). ^{1}H NMR (benzene-d_6): δ = 0.93 (d, 6.8 Hz, 6H, CH(CH_3)$_2$), 1.32 (d, 6.8 Hz, 12H, CH(CH_3)$_2$), 1.37 (d, 6.8 Hz, 6H, CH(CH_3)$_2$), 3.44 (q, 6.8 Hz, 2H, CH(CH$_3$)$_2$), 3.55 (q, 6.8 Hz, 2H, CH(CH$_3$)$_2$), 6.57 (d, 8.0 Hz, 1H, *m-py*), 6.76 (t, 8.0 Hz, 1H, *p-py*), 7.21 (d, 2H, 7.6 Hz, *m-Ar*), 7.26 (d, 2H, 7.6 Hz, *m-Ar*), 7.32 (t, 2H, 7.6 Hz, *p-Ar*), 7.74 (d, 8.0 Hz, 1H, *m-py*), 9.69 (s, 1H, N=CH), one N=CH peak under residual benzene peak. ^{13}C NMR (benzene-d_6): δ = 23.43 (CH(CH$_3$)$_2$), 24.34 (CH(CH_3)$_2$), 27.29 (CH(CH_3)$_2$), 28.32 (CH(CH$_3$)$_2$), 28.83 (CH(CH$_3$)$_2$), 118.30 (*m-py*), 120.72 (*m-py*), 123.56 (*Ar*), 124.16 (*Ar*), 125.48 (*Ar*), 127.17 (*Ar*), 127.73 (*p-py*), 128.92 (*Ar*), 138.72, 141.73, 141.87, 148.90, 150.18, 155.41, 160.77 (quaternary carbons), 164.93 (N=CH), one N=CH peak coincident with the benzene peak.

Preparation of [(^{iPr}PDAI)Fe]$_2$. The arene complex, (^{iPr}PDAI)Fe(η^6-C_7H_8), was generated as described above with 0.500 g (0.747 mmol) of (^{iPr}PDAI)$FeBr_2$, 0.045 g (1.96 mmol) of sodium metal, and 9.00 g (44.9 mmol) of mercury. The resulting crude solid was dissolved in diethyl ether and stored at −35 °C overnight. The solution turned green-brown, and a crystalline solid formed. The crystals were collected and dried and yielded 0.165 g (43%) of a green-brown solid identified as [(^{iPr}PDAI)Fe]$_2$. Crystals suitable for X-ray diffraction were grown from a diethyl ether solution. Analysis for $C_{62}H_{78}N_6Fe_2$: Calcd C, 73.08; H, 7.71; N, 8.25. Found C, 73.16; H, 7.76; N, 7.83. Magnetic susceptibility: μ_{eff} = 4.2 μ_B (Gouy balance, 296 K), μ_{eff} = 4.3 μ_B (SQUID, 300K). ^{1}H NMR (benzene-d_6): δ = −63.59 (50 Hz), −15.43 (15 Hz), −9.82 (42 Hz), −9.76 (26 Hz), −8.58 (13 Hz), −8.18 (20 Hz), −2.25 (17 Hz), −1.86 (17 Hz), −1.60 (22 Hz), 3.93 (19 Hz), 5.01 (16 Hz), 7.55 (21 Hz), 16.62 (15 Hz), 18.26 (106 Hz), 25.86 (25 Hz), 28.03 (18 Hz), 38.95 (25 Hz), 103.76 (27 Hz), 113.62 (35 Hz), 187.33 (158 Hz), 209.28 (61 Hz).

Preparation of (^{iPr}PDAI)Fe(η^4-C_4H_6). A thick-walled glass vessel was charged with 15.00 g (74.78 mmol) of mercury, approximately 30 mL of pentane, and a stir bar. Sodium metal (0.075 g, 3.26 mmol) was added to the vessel. The resulting slurry was stirred for 20 min to amalgamate, then 0.750 g (1.12 mmol) of solid (^{iPr}PDAI)$FeBr_2$ was added to the vessel. The vessel was transferred out of the drybox and submerged in liquid nitrogen. On the high vacuum line, the vessel was evacuated, and 2000 mmHg (10.77 mmol, ∼10 equiv, in 5 × 400 mm portions) of butadiene was added via calibrated gas bulb. The reaction mixture was stirred for 24 h at room temperature during which time the solution changed from blue to orange. After 24 h the excess butadiene was removed on the high vacuum line, and the vessel was brought back into the drybox. The orange solution was decanted away from the amalgam and filtered through Celite. The remaining product was extracted into diethyl ether and also filtered through Celite. Recrystallization from a diethyl ether solution at −35 °C yielded 0.440 g (70%) of a brown solid identified as (^{iPr}PDAI)Fe(η^4-C_4H_6). Crystals suitable for X-ray diffraction were grown from a hexane solution. Analysis for $C_{35}H_{45}N_3Fe$: Calcd C, 74.59; H, 8.05; N, 7.46. Found C, 74.19; H, 7.92; N, 7.18. ^{1}H NMR (benzene-d_6): δ = 0.80 (bs, 6H, CH(CH_3)$_2$), 0.88 (bs, 6H, CH(CH_3)$_2$), 1.12 (bs, 12H, CH(CH_3)$_2$), 1.86 (bs, 2H, CH(CH$_3$)$_2$), 2.54 (bs, 2H, CH(CH$_3$)$_2$), 2.94 (bs, 2H, C_4H_6 CH_2), 3.54 (bs, 2H, C_4H_6 CH_2), 4.59 (bs, 2H, C_4H_6 CH), 6.99 (bs, 6H, *m-* and *p- Ar*), 7.48 (bs, 1H, *p-py*), 7.95 (bs, 2H, *m-py*), 8.43 (bs, 2H, N=CH). ^{1}H NMR (toluene-d_8, −40 °C): δ = 0.80 (d, 6.5 Hz, 6H, CH(CH_3)$_2$), 0.91 (d, 6.5 Hz, 6H, CH(CH_3)$_2$), 1.09 (d, 6.5 Hz, 6H, CH(CH_3)$_2$), 1.14 (d, 6.5 Hz, 6H, CH(CH_3)$_2$), 1.82 (sept, 6.5 Hz, 2H, CH(CH$_3$)$_2$), 2.52 (sept, 6.5 Hz, 2H, CH(CH$_3$)$_2$), 2.78 (m, 2H, C_4H_6 CH_2), 3.39 (d, 12 Hz, 2H, C_4H_6 CH_2), 4.49 (m, 2H, C_4H_6 CH), 6.92 (d, 7.0 Hz, 2H, *m-Ar*), 6.97 (d, 7.0 Hz, 2H *m-Ar*), 7.11 (t, 2H, 7.0 Hz, *p-Ar*), 7.43 (t, 7.5 Hz, 1H, *p-py*), 7.95 (d, 7.5 Hz, 2H, *m-py*), 8.35

(s, 2H, N=C*H*). ^{13}C NMR (benzene-d_6): δ = 22.79 (CH(CH_3)$_2$), 27.02 (CH(CH_3)$_2$), 27.44 (CH(CH_3)$_2$), 28.10 (CH(CH_3)$_2$), 28.65 (CH(CH_3)$_2$), 64.69 (C_4H_6 CH_2), 104.54 (C_4H_6 CH), 118.19 (*m-py*), 123.80 (*m-Ar*), 127.14 (*p-Ar*), 139.00, 147.89, 149.93 (quaternary carbons), 151.07 (N=CH), *p-py* not located.

Preparation of (^{iPr}PDAI)Fe(CO)$_2$. A thick-walled glass vessel was charged with 0.100 g (0.177 mmol) of (^{iPr}PDAI)Fe(η^4-C_4H_6) in 20 mL of diethyl ether. The vessel was evacuated, and one atmosphere of CO was added at liquid nitrogen temperature. The reaction was then warmed to room temperature, and an immediate color change from red-brown to green was observed. The excess CO was removed, and the solution was filtered through Celite. The solvent was removed and yielded 0.092 g (92%) of a green solid identified as (^{iPr}PDAI)Fe(CO)$_2$. Analysis for $C_{33}H_{39}N_3O_2Fe$: Calcd C, 70.09; H, 6.95; N, 7.43. Found C, 69.89; H, 6.95; N, 7.41. ^{1}H NMR (benzene-d_6): δ = 1.01 (d, 6.8 Hz, 12H, CH(CH_3)$_2$), 1.38 (d, 6.8 Hz, 12H, CH(CH_3)$_2$), 2.90 (quint, 6.8 Hz, 4 Hz, C*H*(CH_3)$_2$), 7.16 (m, 6 Hz, *m-* and *p-Ar* and *p-py*), 7.62 (d, 7.6 Hz, 2H, *m-py*), 8.20 (s, 2H, N=C*H*). ^{13}C NMR (benzene-d_6): δ = 23.29 (CH(CH_3)$_2$), 27.66 (CH(CH_3)$_2$), 28.40 (*C*H(CH_3)$_2$), 119.41 (*m-py*), 121.92 (*p-py*), 123.86 (*m-Ar*), 127.65 (*p-Ar*), 141.39, 145.56, 150.58 (quaternary carbons), 152.88 (N=CH). IR(pentane): ν(CO) 1925, 1981 cm^{-1}.

Preparation of (^{iPr}PDAI)Fe(DMAP). A 20 mL scintillation vial was charged with 0.140 g (0.248 mmol) of (^{iPr}PDAI)Fe(η^4-C_4H_6) and approximately 8 mL of diethyl ether. In a second vial, 0.030 g (0.248 mmol) of DMAP was dissolved in approximately 7 mL of diethyl ether. The DMAP solution was then added to the first vial resulting in a change in color from orange to brown. Filtration through Celite and removal of the solvent yielded 0.147 g (95%) of a brown solid identified as (^{iPr}PDAI)Fe(DMAP). Crystals suitable for X-ray analysis were grown from diethyl ether. Analysis for $C_{38}H_{49}N_5Fe$: Calcd C, 72.25; H, 7.82; N, 11.09. Found C, 71.89; H, 7.59; N, 10.92. ^{1}H NMR (benzene-d_6): δ = 0.24 (bs, 6H, CH(CH_3)$_2$), 0.25 (bs, 6H, CH(CH_3)$_2$), 1.22 (bs, 16H, CH(CH_3)$_2$ and C*H*(CH_3)$_2$), 1.90 (bs, 6H, DMAP N(CH_3)$_2$), 5.96 (bs, 2H, DMAP C*H*), 6.82 (bs, 2H, DMAP C*H*), 7.12 (d, 7.6 Hz, 4H, *m-Ar*), 7.59 (t, 7.6 Hz, 2H, *p-Ar*), 8.50 (t, 7.6 Hz, 1H, *p-py*), 12.66 (bs, 2H, *m-py*), 17.16 (bs, 2H, N=C*H*). ^{13}C NMR (benzene-d_6): δ = 22.91 (CH(CH_3)$_2$), 24.51 (CH(CH_3)$_2$), 33.07 (*C*H(CH_3)$_2$), 38.18 (DMAP N(CH_3)$_2$), 97.10 (DMAP *m*-CH), 110.08 (*m-py*), 123.80, 124.19, 124.67, 127.13, 139.10, 152.13, 163.52, 178.39.

■ ASSOCIATED CONTENT

Supporting Information. Representation of the molecular structure of (^{iPr}PDAI). Crystallographic data for (^{iPr}PDAI), (^{iPr}PDAI)Fe(η^4-C_4H_6), (^{iPr}PDAI)Fe(DMAP), and [(^{iPr}PDAI)-Fe]$_2$ in cif format. Additional magnetic data and a representative ^{1}H NMR spectrum of (^{iPr}PDAI)Fe(η^4-C_4H_6). This material is available free of charge via the Internet at http://pubs.acs.org.

■ AUTHOR INFORMATION

Corresponding Author

*E-mail: pchirik@princeton.edu.

Present Addresses

[§]Department of Chemistry, Princeton University, Princeton, New Jersey 08544, United States.

■ ACKNOWLEDGMENT

We thank U.S. National Science Foundation and Deutsche Forschungsgemeinschaft for a Cooperative Activities in Chemistry between U.S. and German Investigators grant. We also thank Dr. Eckhard Bill for insightful discussions about the magnetic data.

■ REFERENCES

(1) For recent reviews see: (a) Bolm, C.; Legros, J.; Paith, J. L.; Zani, L. *Chem. Rev.* **2004**, *104*, 6217. (b) Enthaler, S.; Junge, K.; Beller, M. *Angew. Chem., Int. Ed.* **2008**, *47*, 3317. (c) Correa, A.; Mancheño, O. G.; Bolm, C. *Chem. Soc. Rev.* **2008**, *37*, 1108. (d) Sherry, B. D.; Fürstner, A. *Acc. Chem. Res.* **2008**, *41*, 1500. (e) Bauer, E. B. *Curr. Org. Chem.* **2008**, *12*, 1341. (f) Enthaler, S.; Junge, K.; Beller, M. *Angew. Chem., Int. Ed.* **2008**, *47*, 3317. (g) Gaillard, S.; Renaud, J. L. *ChemSusChem.* **2008**, *1*, 505. (h) Sarhan, A. A. O.; Bolm, C. *Chem. Soc. Rev.* **2009**, *38*, 2730. (i) Morris, R. H. *Chem. Soc. Rev.* **2009**, *38*, 2282. (j) Czaplik, W. M.; Mayer, M.; Cvengros, J.; von Wangelin, J. *ChemSusChem.* **2009**, *2*, 396. (k) Liu, L. X. *Curr. Org. Chem.* **2010**, *14*, 1099.

(2) (a) Small, B. M.; Brookhart, M. *J. Am. Chem. Soc.* **1998**, *120*, 7143. (b) Small, B. L.; Brookhart, M.; Bennett, A. M. A. *J. Am. Chem. Soc.* **1998**, *120*, 4049.

(3) (a) Britovsek, G. J. P.; Gibson, V. C.; Kimberley, B. S.; Maddox, S. J.; Solan, G. A.; White, A. J. P.; Williams, D. J. *Chem. Commun.* **1998**, 849. (b) Britovsek, G. J. P.; Bruce, M.; Gibson, V. C.; Kimberely, B. S.; Maddox, P. J.; Mastroianni, S.; McTavish, S. J.; Redshaw, C.; Solan, G. A.; Strömberg, S.; White, A. J. P.; Williams, D. J. *J. Am. Chem. Soc.* **1999**, *121*, 8728. (c) Gibson, V. C.; Redshaw, C.; Solan, G. A. *Chem. Rev.* **2007**, *107*, 1745.

(4) Bart, S. C.; Lobkovsky, E.; Chirik, P. J. *J. Am. Chem. Soc.* **2004**, *126*, 13794.

(5) Archer, A. M.; Bouwkamp, M. W.; Cortez, M. −P.; Lobkovsky, E.; Chirik, P. J. *Organometallics* **2006**, *25*, 4269.

(6) Russell, S. K.; Darmon, J. M.; Lobkovsky, E.; Chirik, P. J. *Inorg. Chem.* **2010**, *49*, 2782.

(7) Trovitch, R. J.; Lobkovsky, E.; Bill, E.; Chirik, P. J. *Organometallics* **2008**, *27*, 1470.

(8) For olefin hydrogenation with (^{iPr}PDI)Co compounds see: (a) Kooistra, T. M.; Knijnenburg, Q.; Smits, J. M. M.; Horton, A. D.; Budzelaar, P. H. M.; Gal, A. W. *Angew. Chem., Int. Ed.* **2001**, *40*, 4719. (b) Knijnenburg, Q.; Horton, A. D.; van der Heijden, H.; Kooistra, T. M.; Hetterscheid, D. G.; Smits, J. M. M.; de Bruin, B.; Budzelaar, P. H. M.; Gal, A. W. *J. Mol. Catal. A: Chem.* **2005**, *232*, 151.

(9) Bouwkamp, M. W.; Bowman, A. C.; Lobkovsky, E.; Chirik, P. J. *J. Am. Chem. Soc.* **2006**, *128*, 13340.

(10) Sylvester, K. T.; Chirik, P. J. *J. Am. Chem. Soc.* **2009**, *131*, 8772.

(11) Bart, S. C.; Chlopek, K.; Bill, E.; Bouwkamp, M. W.; Lobkovsky, E.; Neese, F.; Wieghardt, K.; Chirik, P. J. *J. Am. Chem. Soc.* **2006**, *128*, 13901.

(12) Bart, S. C.; Lobkovsky, E.; Bill, E.; Wieghardt, K.; Chirik, P. J. *Inorg. Chem.* **2007**, *46*, 7055.

(13) Kuwabara, I. H.; Comninos, F. C. M.; Pardini, V. L.; Viertler, H.; Toma, H. E. *Electrochim. Acta* **1994**, *39*, 2401.

(14) Toma, H. E.; Chavez-Gil, T. E. *Inorg. Chim. Acta* **1997**, *257*, 197.

(15) de Bruin, B.; Bill, E.; Bothe, E.; Weyhermüller, T.; Wieghardt, K. *Inorg. Chem.* **2000**, *39*, 2936.

(16) Budzelaar, P. H. M.; de Bruin, B.; Gal, A. W.; Wieghardt, K.; van Lenthe, J. H. *Inorg. Chem.* **2001**, *40*, 4649.

(17) Knijnenburg, Q.; Gambarotta, S.; Budzelaar, P. H. M. *Dalton Trans.* **2006**, 5442.

(18) Chirik, P. J.; Wieghardt, K. *Science* **2010**, *327*, 794.

(19) Bart, S. C.; Bowman, A. C.; Lobkovsky, E.; Chirik, P. J. *J. Am. Chem. Soc.* **2007**, *129*, 7212.

(20) Bowman, A. C.; Bart, S. C.; Heinemann, F. W.; Meyer, K.; Chirik, P. J. *Inorg. Chem.* **2009**, *48*, 5587.

(21) Knijnenburg, Q.; Hetterscheid, D.; Kooistra, T. M.; Budzelaar, P. H. M. *Eur. J. Inorg. Chem.* **2004**, 1204.

(22) Humphries, M. J.; Tellmann, K. P.; Gibson, V. C.; White, A. J. P.; Williams, D. J. *Organometallics* **2005**, *24*, 2039–2050.

(23) Bowman, A. C.; Milsmann, C.; Atienza, C. C. H.; Lobkovsky, E.; Wieghardt, K.; Chirik, P. J. *J. Am. Chem. Soc.* **2010**, *132*, 1676.
(24) Bowman, A. C.; Milsmann, C.; Bill, E.; Lobkovsky, E.; Weyhermüller, T.; Wieghardt, K.; Chirik, P. J. *Inorg. Chem.* **2010**, *49*, 6110.
(25) Britovsek, G. J. P.; Mastroianni, S.; Solan, G. A.; Baugh, S. P. D.; Redshaw, C.; Gibson, V. C.; White, A. J. P.; Williams, D. J.; Elsegood, M. R. J. *Chem.—Eur. J.* **2000**, *6*, 2221.
(26) Small, B. L.; Brookhart, M. *Macromolecules* **1999**, *32*, 2120.
(27) Gallagher, M.; Wieder, N. L.; Dioumaev, V. K.; Carroll, P. J.; Berry, D. H. *Organometallics* **2010**, *29*, 591.
(28) Bart, S. C.; Hawrelak, E. J.; Lobkovsky, E.; Chirik, P. J. *Organometallics* **2005**, *24*, 5518.
(29) Chaudhuri, P.; Wieghardt, K. *Prog. Inorg. Chem.* **2001**, *50*, 151.
(30) Lu, C. C.; Bill, E.; Weyhermüller, T.; Bothe, E.; Weighardt, K. *J. Am. Chem. Soc.* **2008**, *130*, 3181.
(31) Rochford, J.; Tsai, M. K.; Szaida, D. J.; Boyer, J. L.; Muckerman, J. T.; Fujita, E. *Inorg. Chem.* **2010**, *49*, 860.
(32) Blackmore, K. J.; Sly, M. B.; Haneline, M. R.; Ziller, J. W.; Heyduk, A. F. *Inorg. Chem.* **2008**, *47*, 10522.
(33) The perturbations to the distances in α-iminopyridine ligands may be more appropriate: Lu, C. C.; Weyhermüller, T.; Bothe, E.; Wieghardt, K. *J. Am. Chem. Soc.* **2008**, *130*, 3181.
(34) Andres, H.; Bominaar, E. L.; Smith, J. M.; Eckart, N. A.; Holland, P. L.; Münck, E. *J. Am. Chem. Soc.* **2002**, *124*, 3014.
(35) Freedman, D. E.; Harman, W. H.; Harris, T. D.; Long, G. L.; Chang, C. J.; Long, J. R. *J. Am. Chem. Soc.* **2010**, *132*, 1224.
(36) Borden, W. T.; Iwamura, H.; Berson, J. A. *Acc. Chem. Res.* **1994**, *27*, 109.
(37) Neuhaus, P.; Grote, D.; Sander, W. *J. Am. Chem. Soc.* **2008**, *130*, 2993.
(38) (a) Erker, G.; Kehr, G.; Fröhlich, R. *Adv. Organomet. Chem.* **2004**, *51*, 109. (b) Erker, G.; Kehr, G.; Fröhlich, R. *J. Organomet. Chem.* **2004**, *689*, 4305.
(39) Norman, D. W.; Ferguson, M. J.; McDonald, R.; Stryker, J. M. *Organometallics* **2006**, *25*, 2705.
(40) Bachler, V.; Grevels, F.-W.; Kerpen, K.; Olbrich, G.; Schaffner, K. *Organometallics* **2003**, *22*, 1696.
(41) Trovitch, R. J.; Lobkovsky, E.; Bouwkamp, M. W.; Chirik, P. J. *Organometallics* **2008**, *27*, 6264.
(42) Pangborn, A. B.; Giardello, M. A.; Grubbs, R. H.; Rosen, R. K.; Timmers, F. J. *Organometallics* **1996**, *15*, 1518.
(43) http://ewww.mpi-muelheim.mpg.de/bac/logins/bill/julX_en.php.